

# Supernova Bounds on Resonant Active-Sterile Neutrino Conversions

H. Nunokawa<sup>1 \*</sup>, J. T. Peltoniemi<sup>2 †</sup>, A. Rossi<sup>1 ‡</sup>, and J. W. F. Valle<sup>1 §</sup>

<sup>1</sup>*Instituto de Física Corpuscular - C.S.I.C.*

*Departament de Física Teòrica, Universitat de València*

*46100 Burjassot, València, SPAIN*

*URL <http://neutrinos.uv.es>*

<sup>2</sup>*Department of Physics, Box 9, 00014*

*University of Helsinki, FINLAND*

## Abstract

We discuss the effects of resonant  $\nu_e \rightarrow \nu_s$  and  $\bar{\nu}_e \rightarrow \bar{\nu}_s$  ( $\nu_s$  is a *sterile* neutrino) conversions in the dense medium of a supernova. In particular, we assume the sterile neutrino  $\nu_s$  to be in the hot dark matter few eV mass range. The implications of such a scenario for the supernova shock re-heating, the detected  $\bar{\nu}_e$  signal from SN1987A and for the  $r$ -process nucleosynthesis hypothesis are analysed in some detail. The resulting constraints on mixing and mass difference for the  $\nu_e - \nu_s$  system are derived. There is also an allowed region in the neutrino parameter space for which the  $r$ -process nucleosynthesis can be enhanced.

---

\* E-mail: nunokawa@flamenco.ific.uv.es

† E-mail: Juha.Peltoniemi@Helsinki.fi

‡ E-mail: rossi@gtae2.ist.utl.pt; present address: Dept. de Física, Inst. Superior Tecnico, 1096 Lisbon Codex, Portugal

§ E-mail: valle@flamenco.ific.uv.es

# 1 Introduction

The possibility that light sterile neutrinos can be mixed in the leptonic charged current seems to be the very appealing from the point of view of the present *anomalies* observed in the neutrino sector: the solar [1] and atmospheric [2] neutrino problems as well as the need for a few eV mass neutrino as the hot dark matter in the Universe [3, 4]. Barring the possibility that the three active neutrinos are nearly degenerate in mass [5], the simplest way to simultaneously account for these observations is to postulate <sup>1</sup> the existence of a light sterile neutrino [7, 8, 9]. Moreover, some of these scenarios may also account for neutrino oscillations between the electron neutrino and muon neutrino, as possibly hinted at the LSND experiment [10].

The conversions between neutrino species may change significantly the phenomena occurring in supernova. Of particular interest is the conversion to a sterile neutrino ( $SU(2)_L$  singlet), since the sterile state does not interact at all with the supernova matter.

Here we focus on the resonant conversions of electron neutrinos (or anti-neutrinos) to sterile neutrinos outside the neutrinosphere. For mass difference  $\delta m^2 < 10^4 \text{eV}^2$  the MSW resonance will occur in these regions of the supernova where neutrinos freely stream. Note that for this mass range the conversions to sterile neutrinos in the inner core can be neglected, for all values of the mixing angles [11]. Hence, in the absence of other non-standard interactions, such as a large magnetic moment, the sterile neutrinos are not emitted from the supernova core. We will work always under this assumption. Moreover, we assume that the mass eigenstate consisting mainly of the singlet state is heavier, with mass between 1 eV and 100 eV. The opposite case would require however special forms of the mass matrices in order to avoid the constraints from neutrino-less double beta decay. This possibility certainly exists but, for definiteness we do not consider. Finally, we assume that no other neutrino conversions, such as flavour conversions, take place. Generalization to the case of three-neutrino flavours is straightforward but model-dependent.

The effects of such active to sterile transitions have been previously discussed in [12, 13, 14], mainly concentrating on the effects for neutrino observations at terrestrial detectors. In the present paper we consider the implications of resonant  $\nu_e \rightarrow \nu_s$  or  $\bar{\nu}_e \rightarrow \bar{\nu}_s$  conversions in the dense supernova medium on the neutrino re-heating of the shock wave [15, 16], on the  $\bar{\nu}_e$  signal in terrestrial detectors, as well as on supernova heavy-element nucleosynthesis [17].

The effect of the electron neutrino to sterile neutrino conversion on supernova nu-

---

<sup>1</sup>The measurement of the  $Z$  boson width at LEP has provided a limit on the number of active neutrino types with mass smaller than  $M_Z/2$ ,  $N_\nu = 3.09 \pm 0.13$  [6]. However, it cannot preclude the existence of light sterile neutrinos.

cleosynthesis (via rapid neutron capture process or so-called  $r$ -process) has not yet been discussed with sufficient detail. So far most studies have concentrated on the case of active neutrinos, giving stringent limits on electron, muon and tau neutrino conversions [18, 19]. Nevertheless, it has been suggested [20] that a resonant conversion from muon neutrinos to sterile neutrinos, with a subsequent conversion between electron and muon neutrinos, would enhance  $r$ -process nucleosynthesis. The required conversion pattern appears naturally in some specific models [7].

Neutrino conversions may also influence the explosion mechanisms of the supernova in different ways. Although the main interest lays in the transitions among the active neutrino species [21], it has also been suggested that conversions between sterile and active neutrinos may enhance the explosion [22]. However, for the mass range we are considering, such an enhancement is not possible, the conversions weaken the shock wave, preventing the explosion.

In Sec. 2 we give a quick reminder on the picture of the neutrino propagation in matter and on the resonant  $\nu_e - \nu_s$  conversion [23]. In Sec. 3 we give a qualitative discussion of the electron concentration  $Y_e$  in supernova and on the effects of the active-sterile neutrino conversions on  $Y_e$  and, in turn, on the neutrino evolution itself. This can lead to non-trivial feedback effects [24, 25, 26]. Sec. 4.1 discusses the implications of  $\nu_e - \nu_s$  conversions for the neutrino re-heating mechanism. In Sec. 4.2 we analyse the impact of our scenario in the later epoch of supernova evolution (few seconds after the core bounce) for the supernova (anti)neutrino detection (Sec. 4.2.1) as well as for  $r$ -process nucleosynthesis (Sec. 4.2.2). In Sec. 5 we summarize our results and discuss their significance, by comparing the supernova limits we derive with the laboratory and nucleosynthesis limits on  $\nu_e - \nu_s$  conversions.

## 2 The active-sterile neutrino resonant conversion

In our discussion we only consider the conversion channels  $\nu_e \rightarrow \nu_s$  and  $\bar{\nu}_e \rightarrow \bar{\nu}_s$  where  $\nu_s$  ( $\bar{\nu}_s$ ) is the sterile neutrino <sup>2</sup>. For the sake of simplicity we will not consider the effect of  $\nu_e \leftrightarrow \nu_{\mu,\tau}$  and  $\bar{\nu}_e \leftrightarrow \bar{\nu}_{\mu,\tau}$  conversions. In the following we consider the  $\delta m^2 = m_2^2 - m_1^2 > 0$  case, corresponding (for sufficiently small mixing angle) to the situation in which the heavier state is mostly the sterile neutrino.

The evolution of the  $\nu_e - \nu_s$  system in the matter background is determined by the Schrödinger equation

$$i \frac{d}{dr} \begin{pmatrix} \nu_e \\ \nu_s \end{pmatrix} = \begin{pmatrix} H_e & H_{es} \\ H_{es} & H_s \end{pmatrix} \begin{pmatrix} \nu_e \\ \nu_s \end{pmatrix}, \quad (1)$$

---

<sup>2</sup>In the ultra-relativistic limit  $\nu_s$  and  $\bar{\nu}_s$  have opposite helicity.

$$\begin{aligned}
H_e &= V_e - \frac{\delta m^2}{4E_\nu} \cos 2\theta, & H_s &= V_s + \frac{\delta m^2}{4E_\nu} \cos 2\theta, \\
H_{es} &= \frac{\delta m^2}{4E_\nu} \sin 2\theta,
\end{aligned}
\tag{2}$$

where the effective potential  $V_e$  for  $\nu_e$  arises from the coherent forward neutrino scattering off-matter constituents [23] and is given by <sup>3</sup>

$$\begin{aligned}
V_e &= \frac{\sqrt{2}G_F\rho}{m_N}\left(Y_e - \frac{1}{2}Y_n\right) = \frac{\sqrt{2}G_F\rho}{2m_N}(3Y_e - 1), \\
Y_e &\equiv \frac{n_e}{n_e + n_n}, & Y_n &= 1 - Y_e.
\end{aligned}
\tag{3}$$

Here  $G_F$  is the Fermi constant,  $\rho$  is the matter density,  $m_N$  is the nucleon mass and  $n_e$  and  $n_n$  are the net electron and the neutron number densities in matter, respectively. Note that charge neutrality  $Y_p = Y_e$  is assumed and that there is no potential for  $\nu_s$ , i.e.,  $V_s = 0$ . For the system  $\bar{\nu}_e \rightarrow \bar{\nu}_s$  the matter potentials just change their sign.

The resonance condition reads as:

$$V_e = \frac{\delta m^2}{2E_\nu} \cos 2\theta . \tag{4}$$

Let us remind that for  $\delta m^2 > 0$ , either the conversion  $\nu_e \rightarrow \nu_s$  (for  $V_e > 0$  i.e.  $Y_e > 1/3$ ) or  $\bar{\nu}_e \rightarrow \bar{\nu}_s$  (for  $V_e < 0$  i.e.  $Y_e < 1/3$ ) takes place. This is important because, as we will see later, in the region above the neutrinosphere the matter potential  $V_e$  changes its sign due to the different chemical content. For our later discussion, it is instructive to know the profiles of the matter density and of the electron fraction  $Y_e$  outside the neutrinosphere. In Fig. 1a and 1b we plot these quantities for  $t < 1$  s post-bounce (in short p.b.) and  $t > 1$  s p.b. as given by the Wilson supernova model [27]. We can see that the electron concentration  $Y_e$  is rather low just near the neutrinosphere,  $Y_e \approx 0.1$  and  $0.01$  for the earlier and later epoch, respectively and far away it increases to values  $\gtrsim 0.4$ . On the other hand, the matter density  $\rho$  exhibits a monotonically decreasing behaviour. In Fig. 2a and 2b we plot the modulus of the effective matter potential  $V_e$  using the matter density and  $Y_e$  profiles as given in Fig. 1a and 1b. The position where  $Y_e$  takes the value  $1/3$  (i.e.  $V_e = 0$ ) is indicated by  $r^*$ . This position corresponds to  $r^* \approx 160$  km and  $12$  km for the earlier and later epochs, respectively. Clearly, the effective potential  $V_e$  changes its sign from negative to positive at the point  $r^*$ .

The resonance condition in the eq. (4) provides the  $\delta m^2$  value for which neutrinos with some given energy can experience the resonance for a certain value of the potential

---

<sup>3</sup>The effective potential should also contain contributions from the neutrino background. We have ignored them since the neutrino densities in the relevant regions are at least one order of magnitude smaller than the corresponding electron densities, and the neutrino terms in the effective potential involve an additional suppression factor because most neutrinos travel almost in the same direction.

(or equivalently, at some position  $r$ ). For the sake of convenience, in the right ordinate of Fig. 2 we have also indicated such corresponding values of  $\delta m^2$  for typical neutrino energy  $E = 10$  MeV. We see that for  $\delta m^2 \gtrsim 10^2$  eV<sup>2</sup> only  $\bar{\nu}_e \rightarrow \bar{\nu}_s$  conversions can take place, and this happens in the region where  $Y_e \leq 1/3$ . On the other hand for smaller values,  $\delta m^2 \lesssim 10^2$  eV<sup>2</sup> there can occur three resonances. The  $\bar{\nu}_e$ 's are first converted, say at  $r_1 < r^*$ , then there are two resonance points at  $r_2$  and  $r_3$ , where  $r_3 > r_2 > r^*$  (i.e. in the region where  $Y_e > 1/3$ ), for the  $\nu_e \leftrightarrow \nu_s$  channel. In order to illustrate this more explicitly we plot in Fig. 3 the schematic level crossing diagram for  $\nu_e - \nu_s$  and  $\bar{\nu}_e - \bar{\nu}_s$  system, assuming the mixing angle to be small. From this figure, it is also manifest that the  $\nu_s$ 's originated from the first  $\nu_e$  conversion (at  $r_2$ ) can be re-converted into  $\nu_e$ 's at the second resonance (at  $r_3$ ). In our subsequent discussion, we will employ the simple Landau-Zener approximation [28, 29] to estimate the survival probability after the neutrinos cross the resonance. Under this approximation, the  $\nu_e$  (or  $\bar{\nu}_e$ ) survival probability is given by (in the case of small mixing angle)

$$\begin{aligned}
P &= \exp\left(-\frac{\pi^2}{2} \frac{\delta r}{L_m^{\text{res}}}\right) \\
&\approx \exp\left[-2 \times 10^{-5} \times \sin^2 2\theta \left(\frac{\delta m^2}{\text{eV}^2}\right)^2 \left(\frac{10\text{MeV}}{E_\nu}\right)^2 \left(\frac{dV_e}{dr} \times \frac{\text{km}}{\text{eV}}\right)_{\text{res}}^{-1}\right], \quad (5)
\end{aligned}$$

where  $L_m^{\text{res}}$  is the neutrino oscillation length at resonance. Notice that for  $\delta r/L_m^{\text{res}} > 1$  the resonant neutrino conversion will be adiabatic [23]. We can expect the maximal sensitivity to the mixing angle for  $\delta m^2 = 10^4$  eV<sup>2</sup>. From Fig. 2a and 2b one can estimate that in this case the resonance occurs at high density  $\rho \sim 10^{11} - 10^{13}$  g cm<sup>-3</sup> just above the neutrinosphere, where the gradient  $\frac{dV_e}{dr} \sim 1 - 10^{-2}$  eV km<sup>-1</sup>. From the eq. (5) we can estimate that the conversion will be adiabatic for  $\sin^2 2\theta \gtrsim 10^{-6} - 10^{-4}$ .

Due to the double resonances for the  $\nu_e \leftrightarrow \nu_s$  channel, the  $\nu_e$  survival probability after the second resonance is given by

$$P(\nu_e \rightarrow \nu_e) = P(r_2)P(r_3) + [1 - P(r_2)][1 - P(r_3)], \quad (6)$$

where  $P(r_2)$  and  $P(r_3)$  are the survival probabilities calculated according to the eq. (5) at  $r_2$  and  $r_3$ , respectively.

### 3 The feedback induced by the neutrino conversion

All the neutrino species emitted from the neutrinosphere have approximately the same luminosity  $L_\nu$  after a few ms p.b., characterised by a thermal Fermi distribution with temperature  $T_\nu$  and zero chemical potential. The typical duration of the neutrino emission is about 10 seconds.

### 3.1 Neutrino emission and absorption reactions and $Y_e$ profile in supernova

In the region outside the neutrinosphere, due to the intense neutrino radiation, the electron fraction is determined by the neutrino capture by nucleons and by their reverse processes:

$$\nu_e + n \leftrightarrow p + e^- , \quad (7)$$

$$\bar{\nu}_e + p \leftrightarrow n + e^+ . \quad (8)$$

In particular  $Y_e$  above the neutrinosphere is approximately given by [18]

$$Y_e \approx \frac{\lambda_{e+n} + \lambda_{\nu_e n}}{\lambda_{e-p} + \lambda_{e+n} + \lambda_{\bar{\nu}_e p} + \lambda_{\nu_e n}} . \quad (9)$$

The neutrino capture rates depend essentially on the neutrino luminosity  $L_\nu$  and energy  $E_\nu$ ,

$$\lambda_{\nu N} \approx \int_0^\infty \phi^0(E_\nu) \sigma_{\nu N}(E_\nu) dE_\nu \propto \frac{L_\nu}{\langle E_\nu \rangle} \langle E_\nu^2 \rangle \propto L_\nu \langle E_\nu \rangle , \quad (10)$$

where  $(\nu, N) = (\nu_e, n)$  or  $(\bar{\nu}_e, p)$ . The neutrino luminosity is given by the black-body surface emission formula,  $L_\nu = 5.6 \times 10^{46} r_\nu^2 T_\nu^4$  ergs/s (here  $r_\nu$  is given in km and  $T_\nu$  in MeV). For our purpose it is sufficiently accurate to assume the neutrino differential flux  $\phi^0(E_\nu)$  to be given by

$$\phi^0(E_\nu) = \frac{L_\nu}{4\pi r^2} \frac{E_\nu^2 / (e^{E_\nu/T_\nu} + 1)}{\int E_\nu^3 dE_\nu / (e^{E_\nu/T_\nu} + 1)} . \quad (11)$$

On the other hand, the rates for the inverse processes depend strongly on the matter temperature  $T$  and are given as

$$\lambda_{eN} \approx \frac{1}{\pi^2} \int_0^\infty \frac{\sigma_{eN}(E_e) E_e^2}{\exp[(E_e \mp \mu_e)/T] + 1} dE_e \propto T^5 , \quad (12)$$

where  $\sigma_{eN}$  is the electron or positron capture cross section with  $(e, N) = (e^-, p)$  or  $(e^+, n)$ . (In the above formula the negative sign in front of  $\mu_e$  is for electrons and the positive sign is for positrons.)

In Fig 4a and 4b we have plotted the above rates  $\lambda_{\nu N}, \lambda_{eN}$  (for the earlier and later epochs, respectively) as a function of the distance from the centre of the star. For convenience we have also plotted the matter temperature profile by the solid line (see the right ordinate scale). One can see from Fig. 4a and 4b that close to the neutrinosphere the rate  $\lambda_{e-p}$  dominates over the others, and hence  $Y_e$  is less than 1/3 (see the eq. (9)), as can be seen from Fig. 1a and 1b. As  $r$  increases  $\lambda_{e-p}$  decreases faster than  $\lambda_{\nu N}$  and hence  $Y_e$  increases. At some point  $r \sim r^*$  where  $\lambda_{e-p} \sim \lambda_{\nu N}$ , the fraction  $Y_e$  takes the value 1/3. In the region  $r > r^*$  where the neutrino absorption reaction is high enough to dominate the

proton-to-neutron ratio, the electron fraction is given by

$$Y_e \approx \frac{\lambda_{\nu_e n}}{\lambda_{\bar{\nu}_e p} + \lambda_{\nu_e n}} \approx \frac{1}{1 + \langle E_{\bar{\nu}_e} \rangle / \langle E_{\nu_e} \rangle}. \quad (13)$$

assuming the fluxes to be given as in the eq. (11). For the typical energies  $\langle E_{\nu_e} \rangle \sim 11$  MeV and  $\langle E_{\bar{\nu}_e} \rangle \sim 16$  MeV at  $t > 1$  s p.b., we find  $Y_e = 0.41$ , in good agreement with numerical supernova models [18]. The above discussion explains well the behaviour of the  $Y_e$  profiles shown in Fig. 1a and 1b.

### 3.2 Feedback effect on neutrino conversion

Now let us come to the main point concerning the effect of the neutrino conversion upon the electron content in the matter. Suppose that at some position  $r_0$  and time  $t_0$  neutrino conversions  $\nu_e \rightarrow \nu_s$  or  $\bar{\nu}_e \rightarrow \bar{\nu}_s$  occur. From the eq. (4) and eq. (5) we see that the conversion probability depends on the value of  $Y_e$  and its derivative at the resonance position  $r_0$ . The neutrino conversions  $\nu_e \rightarrow \nu_s$  or  $\bar{\nu}_e \rightarrow \bar{\nu}_s$  reduce the value of  $\lambda_{\nu_e n}$  or  $\lambda_{\bar{\nu}_e p}$  and this could lead to the modification of  $Y_e$  in the region  $r > r_0$  (see the eq. (9)). If the modification of  $Y_e$  is fast enough it could affect any subsequent neutrino conversion occurring at some position  $r > r_0$  and time  $t > t_0$ . This subsequent neutrino conversion could again modify the value of  $Y_e$ , and so on. In this way, neutrino conversion rates and the electron fraction continuously affect each other during the neutrino emission, leading to non-trivial feedback phenomena for the neutrino transitions. These should in principle be taken into account self-consistently in neutrino conversion studies. It is well known that in the early universe feedback effects on the neutrino background should be reflected in the evolution of neutrinos [24] and such effects have been studied in ref. [25]. On the other hand, in the context of supernova physics, feedback effects on the neutrino background have recently been studied in ref. [26]. In what follows we will consider the analogous effect for the electron abundance  $Y_e$ .

From our discussion in Sec. 3.1, we can immediately understand that the feedback is operative only when  $\lambda_{\nu N} \gg \lambda_{eN}$  (see the eq. (9)). Right after the bounce ( $t < 1$  s p.b.) the relevant resonance layers lie so far away from the stellar core that the  $\lambda_{\nu N}$  is too small since  $\phi^0 \propto r_v^2/r^2$  (cfr. eq. (11)) and as a result feedback effects would be small. On the other hand, later on ( $t > 1$  s p.b.) the neutrinosphere shrinks so much that  $\lambda_{\nu N}$  is high at the relevant resonance positions (now they lie much closer to the centre) and, as a result, the feedback effects would be potentially important.

The neutrino conversion could be affected by the feedback either by shifting of the resonance position, or through a change in the adiabaticity. Let us first see the effect on the resonance position. For simplicity let us assume that  $Y_e$  is determined only by  $\lambda_{\nu N}$  as in eq. (13). In the region where  $Y_e > 1/3$  ( $Y_e < 1/3$ ) the  $\nu_e \rightarrow \nu_s$  ( $\bar{\nu}_e \rightarrow \bar{\nu}_s$ ) conversions

occur and this tends to decrease (increase)  $Y_e$  in the region above the resonance layer because  $\lambda_{\nu_e n}$  ( $\lambda_{\bar{\nu}_e p}$ ) decreases. This could affect the resonance condition for the subsequent neutrinos, leading to a shift of the resonance position. Moreover, if the value of  $Y_e$  becomes less or equal to  $1/3$ , the subsequent  $\nu_e \rightarrow \nu_s$  conversion would be suppressed because the resonance condition is not satisfied. This is therefore a negative feedback. Analogously, a negative feedback is also present for the  $\bar{\nu}_e \rightarrow \bar{\nu}_s$  channel.

Let us now turn to the feedback effect on the adiabaticity. The neutrino conversion would change the potential gradient gradually, as neutrinos of different parts of the energy spectra reach the resonance. In the case of  $\bar{\nu}_e \rightarrow \bar{\nu}_s$  conversion, the depletion of the anti-neutrino flux drives  $Y_e$  up by decreasing the anti-neutrino capture rate, and so it tends to raise the absolute value of the gradient of the potential. This weakens the adiabaticity of the neutrino conversion. As for the  $\nu_e \rightarrow \nu_s$  conversion, in the increasing part of the potential in Fig. 2, due to the decrease of  $Y_e$  caused by  $\nu_e$  to  $\nu_s$  conversion, the shape of the potential would be flattened, leading to better adiabaticity. On the other hand, for the decreasing part of the potential (see again Fig. 2), the potential gradient would be steepened leading to worse adiabaticity.

Let us now consider the relevance of the feedback in terms of the  $\delta m^2$  involved. We can distinguish three different ranges of  $\delta m^2$ : (i)  $10^3 \text{ eV}^2 < \delta m^2 < 10^4 \text{ eV}^2$ , (ii)  $10^2 \text{ eV}^2 < \delta m^2 < 10^3 \text{ eV}^2$  and (iii)  $\delta m^2 < 10^2 \text{ eV}^2$ . For the mass range (i) and (ii) (see Fig. 2), only anti-neutrino conversions take place, while for the range (iii) both neutrino and anti-neutrino conversions take place. In range (i), the transitions occur close enough to the neutrino sphere, where the  $e^- p \rightarrow \nu_e n$  reaction dominates over the corresponding neutrino absorption reactions. In this case  $Y_e$  around the resonance position is not affected by the  $\bar{\nu}_e \rightarrow \bar{\nu}_s$  conversion. Hence the feedback is irrelevant for this mass range.

On the other hand, for the range (ii), the conversions occur farther away from the neutrinosphere where the  $e^- p \rightarrow \nu_e n$  rate becomes comparable to that of  $\bar{\nu}_e p \rightarrow e^+ n$ , especially in the later epoch. Hence the anti-neutrino conversion would be somewhat more affected by the feedback than in the previous case. However, the effect is still not large, since  $\lambda_{e^- p}$  is not small compared to  $\lambda_{\nu N}$ .

Finally, for the range (iii) the situation is more complicated. In this case three resonant conversions can occur: one in the  $\bar{\nu}_e \rightarrow \bar{\nu}_s$  channel and two in the  $\nu_e \leftrightarrow \nu_s$  channel (see Fig. 3). For the  $\bar{\nu}_e \rightarrow \bar{\nu}_s$  resonant conversion (at  $r_1 < r^*$ ) the preceding conclusion still holds and the feedback is not important. Similarly the next conversion  $\nu_e \rightarrow \nu_s$  (at  $r_2 > r^*$ ) is not too affected by the feedback due to its proximity to the core, as before. Moreover, this  $\nu_e \rightarrow \nu_s$  conversion is expected to have the same degree of adiabaticity as that of the previous anti-neutrino conversion, due to roughly the same steepness of the matter potential. As a result  $P(\bar{\nu}_e \rightarrow \bar{\nu}_s; r_1) \approx P(\nu_e \rightarrow \nu_s; r_2)$  and, to some extent the



change in  $Y_e$  at  $r_2$  will be compensated by that at  $r_1$ , leading to a small net feedback <sup>4</sup>.

Now let us come to the last resonance in the channel  $\nu_e \leftrightarrow \nu_s$ , at  $r_3$ . This conversion could be significantly affected by the feedback because in the region around  $r_3$  ( $\gg r^*$ )  $Y_e$  is determined only by the  $\lambda_{\nu N}$  reaction rates, since the inverse rates are small, as seen from Fig. 4b. For the sake of discussion, let us first consider the case where the conversions at  $r_1$  and  $r_2$  are sufficiently adiabatic. In this case the resonance at  $r_3$  is also expected to be very adiabatic, since the slope of the potential around  $r_3$  is much less steep than that for the previous resonances. Therefore, the  $\nu_e$  flux would be completely recovered by the last conversion  $\nu_s \rightarrow \nu_e$  at  $r_3$ . This last conversion  $\nu_s \rightarrow \nu_e$  would remain adiabatic because the increase of  $Y_e$  due to the conversion would not violate the adiabaticity but simply shift the resonance position. As a result we conclude that it would not be affected by the feedback. In the opposite case, when at  $r_1$  and  $r_2$  the conversions are not adiabatic ( $P \sim 1$ ), the feedback effect, due to the last  $\nu_e \leftrightarrow \nu_s$  transitions, could be very important. The depletion of the electron neutrino flux and the unchanged  $\bar{\nu}_e$  flux would lower the value of  $Y_e$  and hence  $V_e$ , with the effect of shifting the resonance position  $r_3$  at lower values. At the same time the potential gradient becomes steeper and hence the conversions become less adiabatic, leading to the suppression of the  $\nu_e \rightarrow \nu_s$  transition. In this case we would have a net feedback effect on the neutrino conversion. This situation occurs for rather small mixing angle  $\sin^2 2\theta < 10^{-2}$  and for  $\delta m^2 < 10^2 \text{ eV}^2$ . We can have a quantitative insight of the significance of the effect from the eq. (13) by simply requiring  $Y_e \geq 1/3$ . For simplicity, let us assume  $P_{\bar{\nu}_e}(r_1) \sim P_{\nu_e}(r_2) \sim 1$ . Thus we can deduce a lower bound for the survival probability at  $r_3$ ,  $P_{\nu_e}(r_3) \gtrsim 0.7$ . In other words, the second  $\nu_e \rightarrow \nu_s$  conversion would be stopped when about 30 % of the lower part of  $\nu_e$  spectra are converted to  $\nu_s$  (because the lower energy neutrinos undergo resonance before the higher ones) even if the conversion is initially very adiabatic.

Instead of taking into account this feedback effect upon the neutrino evolution, we have simply stop the  $\nu_e \rightarrow \nu_s$  conversion when  $Y_e$  reaches the value of  $1/3$ .

We conclude that the feedback effects would be small and could be neglected in the earlier epoch in the region relevant for our discussion. As for the later epoch, the feedback may be more relevant especially for the range  $\delta m^2 < 10^2 \text{ eV}^2$ .

---

<sup>4</sup>This observation is strictly true in the case of absence of the feedback. However, since the feedback effect may slightly decrease the adiabaticity of anti-neutrinos and increase the adiabaticity of neutrinos, the conversion probability for neutrinos may be a little larger than for anti-neutrinos.

## 4 Constraining Neutrino Parameters

In this section we are mainly concerned with the implications of active-sterile neutrino conversions for supernova physics. For the earlier epoch of supernova evolution active-sterile neutrino conversions would suppress the shock re-heating. For the later epoch active-sterile neutrino conversions could suppress the detected  $\bar{\nu}_e$  signal from SN1987A. On this basis we derive stringent constraints on the neutrino parameters. On the other hand, these conversions could affect the  $r$ -process nucleosynthesis in the later epoch, either to suppress it or to enhance. In the first case we again analyse the restrictions on neutrino parameters.

### 4.1 Earlier Epoch: $t < 1$ second after core bounce

In the following we consider only the epoch after the core bounce and the neutrino evolution in the regions outside its neutrinosphere. Indeed, for the range  $\delta m^2 \leq 10^4$  eV<sup>2</sup> neutrino transitions in the dense matter of the core ( $\rho \sim 10^{13}$  g/cm<sup>3</sup>) are strongly suppressed [11, 13].

At this time a *reflected* shock wave is formed between the inner homologously collapsing part and the supersonically falling outer portion of the initial iron core. This shock propagates through the mantle and may result in mass ejection when it reaches the surface of the star. In fact the shock suffers energy loss due in particular to the emission of neutrinos which prevents a successful explosion of the star. As soon as the shock wave has passed through the neutrinosphere there is a large burst of  $\nu_e$ 's. Subsequently on a time scale of several seconds after the core bounce the emission of all neutrino species drives the evolution of the star to the final cool and neutron star. The epoch within 1 second after the core bounce is rather important for the re-heating of the shock wave. In the delayed explosion mechanism [15, 16] the neutrino energy deposition, occurring between the neutrino sphere and the site where the shock is stalled, can re-start the shock and power the explosion. As can be seen from Fig. 4a, at  $r \sim 300 \div 400$  km away from the neutrinosphere the neutrino absorption rate on free nucleons dominates over the capture of electrons. At this position the energy transfer from neutrinos to the matter takes place so as to help the shock <sup>5</sup>.

In the absence of neutrino conversions the corresponding energy gain (per nucleon)

$\frac{dE}{dt} \equiv \dot{E}(t)$  is

$$\dot{E}(t) \approx \frac{L_\nu \sigma_{\nu N}}{4\pi r^2} \quad (14)$$

where  $L_\nu$  is the total  $\nu_e + \bar{\nu}_e$  luminosity and  $\sigma_{\nu N} \sim 9 \times 10^{-44} \times E_\nu^2$  cm<sup>2</sup>. For  $L_\nu \sim 3 \times 10^{52}$

---

<sup>5</sup>Other mechanisms for energy deposition, like neutrino scattering off-electrons or neutrino-anti-neutrino annihilation are less efficient [30] and thereby we neglect them in the following.

ergs/s,  $E_\nu = 10$  MeV and  $r = 300$  km, we find  $\dot{E}(t) \sim 20$  MeV s<sup>-1</sup>. This rate seems to be large enough on the time scale of 0.1-0.2 second if compared with the gravitational potential (per unit mass)  $G_N M_r / r \sim 7$ -10 MeV of the material stopped behind the shock ( $M_r \sim 1.5 M_\odot$  is the included mass). Thus the neutrino energy transfer can help the material to overcome the gravitation of the star and so to escape it. The success of this scenario strongly depends on the neutrino luminosity. Clearly the sterile conversion  $\nu_e \rightarrow \nu_s$  or  $\bar{\nu}_e \rightarrow \bar{\nu}_s$  would imply a depletion of active neutrino luminosity and thereby can spoil the re-heating process [13].

We have calculated the ratio  $R$  of the neutrino heating rate in the presence of  $\nu_e \rightarrow \nu_s$  and  $\bar{\nu}_e \rightarrow \bar{\nu}_s$  transitions to the corresponding rate in the absence of such transitions. Following ref. [16] we use an approximate expression for  $R$ , in which we neglect the re-emission of neutrinos by the heated matter, leading to

$$R = \frac{Y'_n \dot{E}'_{\nu_{en}}(t) + Y'_p \dot{E}'_{\bar{\nu}_{ep}}(t)}{Y_n \dot{E}_{\nu_{en}}(t) + Y_p \dot{E}_{\bar{\nu}_{ep}}(t)} , \quad (15)$$

$$\dot{E}_{\nu N}(t) \sim \int E_\nu \sigma_{\nu N} \phi^0(E_\nu) dE_\nu , \quad \dot{E}'_{\nu N}(t) \sim \int E_\nu \sigma_{\nu N} P(E_\nu) \phi^0(E_\nu) dE_\nu . \quad (16)$$

where the primed quantities  $Y'_p$  and  $Y'_n$  stand for the proton and neutron abundances calculated in the presence of active-sterile neutrino conversions.

In Fig. 5 we plot the iso-contour for different values of the ratio  $R$  in the parameter space  $(\delta m^2, \sin^2 2\theta)$ . Requiring a moderate effect  $R > 0.9$ , one can exclude  $\sin^2 2\theta > 10^{-8}$  for  $\delta m^2 \sim 10^4$  eV<sup>2</sup>, whereas for smaller mass,  $\delta m^2 \sim 1 \div 10$  eV<sup>2</sup>, the bound on the mixing is weaker and lies in the range  $\sin^2 2\theta > 7 \times 10^{-5} \div 5 \times 10^{-3}$ . Note that our bounds are in qualitative agreement, though slightly more stringent than those found e.g. in ref. [13].

## 4.2 Later Epoch: $t > 1$ second after core bounce

For the later epoch we consider the effect of active-sterile neutrino conversions both on the  $\bar{\nu}_e$  signal as well as the  $r$ -process nucleosynthesis and analyse the possible restrictions on neutrino parameters.

### 4.2.1 Implications for the detection of SN1987A $\bar{\nu}_e$ signal

The Kamiokande II and IMB detectors observed 11 and 8  $\bar{\nu}_e$  events, respectively, from SN1987A [31, 32]. This is in agreement with the theoretical expectations, which predict that almost all of the released gravitational energy is radiated in all neutrino and anti-neutrino flavours. Significant conversion of  $\bar{\nu}_e$ 's into a sterile neutrino would be in conflict with this evidence. We can just apply this consideration to constrain the neutrino mixing and mass difference.

We plot in Fig. 6 three contours of the  $\bar{\nu}_e$  survival probability  $P$  for the  $\bar{\nu}_e \rightarrow \bar{\nu}_s$  conversion, in the  $(\delta m^2, \sin^2 2\theta)$  parameter space. The upper line is for  $P = 0.1$ , the lower one is for  $P = 0.7$  and that in the middle corresponds to  $P = 0.5$ . If we assume that the successful observation of the SN1987A signal implies that at least 50 % of the expected  $\bar{\nu}_e$  signal has been detected, one can conclude that all the portion above the contour of  $P = 0.5$  is ruled out. For  $\delta m^2 = 10^4 \text{ eV}^2$ , the range  $\sin^2 2\theta > 5 \times 10^{-6}$  is excluded whereas for  $\delta m^2 = 1 \div 10 \text{ eV}^2$  the non-adiabatic character of the conversion implies a much looser bound,  $\sin^2 2\theta \geq 10^{-1}$ . Our results are again in qualitative agreement with those in [12, 13].

Now we would like just to briefly comment on the relevance of the large volume detectors, such as Superkamiokande [33] or SNO [34], aimed to detect supernova neutrinos. A galactic supernova event would produce e.g. about 5000 events through  $\bar{\nu}_e p$  reaction in Superkamiokande detector. Such a huge statistics may not only allow to determine the neutrino flux with good accuracy but also may provide the necessary sensitivity to measure e.g. the neutrino energy spectrum. The resonant conversion between electron neutrinos and sterile neutrinos may show up as a deficit of neutrino events, distortion of spectra, time dependent flux, etc. The absence of a deficit in the expected number of events can be used to further constrain the neutrino parameters. In Superkamiokande detector a number of  $\bar{\nu}_e$  events not larger than 2500 would disfavour all the region above the iso-contour of  $P = 0.5$  in Fig. 6. However the observation of a possible deficit on electron neutrinos or anti-neutrinos is not in itself a distinguishable signal for any specific conversion mechanism. Moreover, the precision of any conclusions that can be drawn from these considerations is limited by the uncertainties in the theoretical neutrino fluxes.

A better signal is the distortion of the neutrino energy spectrum that would arise from the neutrino conversion. The energy dependence of the adiabaticity condition may already cause a mild distortion, typically neutrinos of lower energies have larger conversion probabilities. That is, however, a general feature of the resonant conversion irrespective of the specific neutrino channel. However, we can envisage a possible distortion caused by the feedback effect. As discussed in Sec. 3, the feedback effect may cause a 30 % reduction of neutrino events in the low-energy portion of the neutrino spectrum (with a sharp cutoff energy close to 10 MeV). In other words, there will be a tendency for neutrinos above this energy to be blocked from converting. In order for this to happen, the following conditions are to be satisfied: 1) the first resonances (for electron neutrinos and anti-neutrinos) must be non-adiabatic i.e. for  $\delta m^2 < 10^2 \text{ eV}^2$ ,  $\sin^2 2\theta < 10^{-2}$ ; 2) the last resonance should be in the region where the electron fraction is determined by the neutrino absorption reactions, i.e. for  $\delta m^2 > 1 \text{ eV}^2$ ; 3) the last resonance should be adiabatic. A more detailed and careful analysis will be given elsewhere[35].

## 4.2.2 Implications for $r$ -process Nucleosynthesis

The implications of resonant neutrino conversions into active neutrinos for the supernova nucleosynthesis have been recently investigated in a number of papers [18, 19].

The  $r$ -process is responsible for synthesising about half of the heavy elements with mass number  $A > 70$  in nature. It has been proposed that the  $r$ -process occurs in the region above the neutrinosphere in supernovae when significant neutrino fluxes are still coming from the neutron star [17]. A necessary condition required for the  $r$ -process is  $Y_e < 0.5$  in the nucleosynthesis region. The  $Y_e$  value at large radii above the neutrinosphere, where the  $r$ -process nucleosynthesis takes place, is determined, as we have discussed in Sec. 3, only by the neutrino absorption rates  $\lambda_{\nu_e n}$  and  $\lambda_{\bar{\nu}_e p}$ . Therefore,  $Y_e$  in the nucleosynthesis region is approximately given by the eq. (13). We have also learnt that the presence of neutrino conversions into a sterile state can affect the corresponding  $Y_e$ . Thereby, in the nucleosynthesis region we can write  $Y_e$  as follows

$$Y_e \approx \frac{1}{1 + P_{\bar{\nu}} \langle E_{\bar{\nu}_e} \rangle / P_{\nu} \langle E_{\nu_e} \rangle}, \quad (17)$$

As we already noted the  $\bar{\nu}_e \rightarrow \bar{\nu}_s$  conversion leads to a reduction of  $\bar{\nu}_e$  luminosity and hence to an increase of  $Y_e$ , whereas the  $\nu_e \rightarrow \nu_s$  conversion acts in the opposite way. Depending on the  $\delta m^2$  range, one channel dominates over the other one. For  $\delta m^2 \geq 10^2 \text{ eV}^2$ , only  $\bar{\nu}_e \rightarrow \bar{\nu}_s$  can occur which increases  $Y_e$  with respect to the case with no anti-neutrino conversion. For smaller values of  $\delta m^2$  there is an interplay of both conversions  $\bar{\nu}_e \rightarrow \bar{\nu}_s$  and  $\nu_e \rightarrow \nu_s$  which can make  $Y_e < 0.4$ , hence enhancing the  $r$ -process.

Properly averaging the neutrino absorption rates over the neutrino Fermi distribution, we have calculated the electron abundance  $Y_e$  at the site where the heavy elements nucleosynthesis should take place as a function of  $(\delta m^2, \sin^2 2\theta)$ . In Fig. 7 we present our result.

For a successful  $r$ -process, the region above  $Y_e > 0.5$  is ruled out. For  $\delta m^2 \geq 10^2 \text{ eV}^2$  and  $\sin^2 2\theta > 2 \times 10^{-6} - 10^{-5}$  only the  $\bar{\nu}_e \rightarrow \bar{\nu}_s$  channel undergoes the conversion. As we have discussed in Sec. 4, this region is also disfavoured by the neutrino re-heating consideration (Fig. 5). In correspondence of the corner delimited by  $50 \text{ eV}^2 \leq \delta m^2 \leq 10^2 \text{ eV}^2$  and  $\sin^2 2\theta > 10^{-3}$  the conversions take place in both channels  $\bar{\nu}_e \rightarrow \bar{\nu}_s$  and  $\nu_e \leftrightarrow \nu_s$  and are adiabatic enough. In this case the significant suppression of the  $\bar{\nu}_e$  flux and the recovery of the original  $\nu_e$  flux at  $r_3$  would lead to  $Y_e > 0.5 - 1$ .

On the other hand we find that the supernova nucleosynthesis could be enhanced in the region enclosed by the dotted contour  $Y_e = 0.4$ , delimited by  $\delta m^2 \leq 10^2 \text{ eV}^2$  and  $\sin^2 2\theta \geq 10^{-5}$ . Inside the contour of  $Y_e = 0.33$ ,  $Y_e$  gets stabilised to  $1/3$  due to the feedback effect (in the absence of the feedback  $Y_e$  would be lower than  $1/3$  - see the discussion in Sec. 3.2). We see that the mass range more promising for the neutrino hot

dark matter scenario,  $\delta m^2 \leq 10 \text{ eV}^2$ , is favourable for the  $r$ -process nucleosynthesis and it is neither in conflict with the re-heating process (see Fig. 5) nor with SN1987A observations (see Fig. 6).

## 5 Discussion

In this paper we have investigated the effect of resonant conversions of  $\nu_e$  or  $\bar{\nu}_e$  into sterile neutrinos in the region above the hot proto-neutron star in type II supernova. For cosmologically interesting mass values (1-100 eV) and mixing angle  $\sin^2 2\theta \gtrsim 10^{-7} \div 10^{-5}$ , both  $\nu_e$  and  $\bar{\nu}_e$  could be converted into  $\nu_s$  and  $\bar{\nu}_s$  (respectively) in the region outside neutrinosphere due to the non-monotonic behaviour of the effective matter potential. Such conversion could lead to the depletion of  $\nu_e$  and  $\bar{\nu}_e$  fluxes, resulting in a suppression of the neutrino re-heating behind the stalled shock and of the expected  $\bar{\nu}_e$  signal in terrestrial detectors. On the basis of these arguments we have derived constraints the neutrino mass and mixing parameters. We have found that for  $\delta m^2 \sin^2 2\theta \gtrsim 10^{-3} \text{ eV}^2$ , the energy deposition by  $\nu_e$  and  $\bar{\nu}_e$  absorption reactions during the shock re-heating epoch ( $t < 1$  s after the bounce) could be significantly decreased. This is not welcome for the delayed explosion scenario which relies on the revival of the shock by neutrino re-heating.

The successful observation of the SN1987A  $\bar{\nu}_e$  signal in the IMB and Kamiokande detector can also be used in order to rule out a similar parameter range. Indeed, requiring that the total  $\bar{\nu}_e$  flux during the thermal neutrino emission epoch ( $t \sim 1 - 10$  s p.b.) should not be significantly depleted by  $\bar{\nu}_e \rightarrow \bar{\nu}_s$  conversion enables us to rule out the range  $\delta m^2 \sin^2 2\theta \gtrsim 10^{-1} \text{ eV}^2$ .

We further point out that depending on which conversion channel,  $\nu_e \rightarrow \nu_s$  or  $\bar{\nu}_e \rightarrow \bar{\nu}_s$  is dominant,  $r$ -process nucleosynthesis, which might take place in neutrino-heated supernova ejects at  $1 < t \lesssim 20$  s p.b., could either be suppressed or enhanced. For the parameter range  $\delta m^2 \sin^2 2\theta \gtrsim 10^{-1} \text{ eV}^2$  where  $\bar{\nu}_e \rightarrow \bar{\nu}_s$  conversion is dominant,  $Y_e$  at the nucleosynthesis site could become larger than 0.5 and hence  $r$ -process would be prevented, leading to the exclusion of this range of mass and mixing. On the other hand,  $r$ -process nucleosynthesis could be enhanced due to the decrease of  $Y_e$  down to the minimum value 1/3. This is due to the fact that the  $\nu_e \rightarrow \nu_s$  conversion is dominant if the parameters are in the region  $\delta m^2 \lesssim 100 \text{ eV}^2$  and  $\sin^2 2\theta \gtrsim 10^{-5}$ .

We have also discussed that, in contrast to the usual resonant conversion among active neutrinos (such as  $\nu_e \leftrightarrow \nu_\mu, \nu_\tau$ ), the decrease or increase of  $Y_e$  due to  $\nu_e \rightarrow \nu_s$  or  $\bar{\nu}_e \rightarrow \bar{\nu}_s$  conversion could be important in the estimation of the conversion probabilities. Indeed, the conversion could be suppressed when  $Y_e$  reaches a value close to 1/3. Such effect may take place both for  $\nu_e \rightarrow \nu_s$  or  $\bar{\nu}_e \rightarrow \bar{\nu}_s$  resonant conversions. However, such

feedback effect should not be operative when the conversion occurs in the region where the electron or positron capture reaction is dominant over the neutrino absorption reaction, or if both conversions ( $\nu_e$  and  $\bar{\nu}_e$  channels) occur in the same region.

Finally, we wish to remark on the importance of the supernova constraints on active sterile neutrino conversions we have derived here. Most high-energy particle physics experiments are insensitive to the possible existence of sterile neutrinos since these do not couple to the electroweak currents. However, their admixture in the charged current weak interaction could show up in reactor neutrino disappearance searches. The laboratory limits on the mixing between electron neutrinos and sterile neutrinos are quite weak for this mass range. From reactor experiments the bound is weaker than  $\sin^2 2\theta \lesssim 0.01$  [36], far weaker than the supernova limits we derive. In contrast, for large mixing the reactor limit on  $\delta m^2 \lesssim 10^{-2} \text{ eV}^2$  is stronger than the corresponding supernova limits.

A much stronger though also more uncertain argument to constrain active-sterile neutrino conversions comes from big-bang cosmological nucleosynthesis. Assuming that the number of effective neutrino species is bounded to be less than 4, one has [37]:

$$\delta m^2 \sin^4 2\theta \lesssim 5 \times 10^{-6} \text{ eV}^2, \quad \nu = \nu_e, \quad (18)$$

$$\delta m^2 \sin^4 2\theta \lesssim 3 \times 10^{-6} \text{ eV}^2, \quad \nu = \nu_\mu, \nu_\tau. \quad (19)$$

However the recent discrepant observational determinations of the primordial deuterium abundances [40, 41] may force us to revise big-bang nucleosynthesis constraints on nonstandard neutrino physics. As a result the assumptions on which the previous limit is based are under debate [38]. It has been argued that  $N_\nu > 4$  is acceptable [39], in which case there would be room to bring an extra sterile neutrino species into equilibrium with the known neutrinos in the early Universe and therefore no constraints on active to sterile neutrino oscillation parameters. Therefore, from this point of view, the restrictions on active-sterile neutrino oscillation parameters obtained from supernova theory and observations become quite relevant.

### Acknowledgement

We thank Y.-Z. Qian for stressing to us the importance of feedback effects in supernovae and for a helpful discussion. This work has been supported by DGICYT under Grant N. PB95-1077, by a joint CICYT-INFN grant, and by the TMR network ERBFM-RXCT960090 of the European Union. H. N. has been supported by Ministerio de Educación y Ciencia and A. R. by the Human Capital and Mobility Program under Grant No. ERBCHBI CT-941592 and by the Grupo Teorico de Altas Energias at Instituto Superior Tecnico (Lisboa). A. R. thanks the CERN Theory Division for hospitality during part of this work. H. N. thanks the Institute for Nuclear Theory at the University of Washington for its hospitality during the part of this work.

## References

- [1] B.T. Cleveland *et al.*, Nucl. Phys. B (Proc. Suppl.) **38**, 47 (1995); GALLEX Coll., Phys. Lett. **B388**, 384 (1996); Gavrin (SAGE Collaboration), talk presented at the *Neutrino 96* Conf, Helsinki, 1996 to appear in the Proc. Neutrino 96, Helsinki, ed. K. Huitu, K. Enqvist and J. Maalampi (World Scientific, Singapore, 1997); Kamiokande Collaboration, Phys. Rev. Lett. **77**, 1683 (1996).
- [2] Kamiokande Collaboration, Phys. Lett. **B335**, 237 (1994); IMB Collaboration, Phys. Rev. Lett. **66**, 2561 (1989); Soudan 2 Collaboration, Nucl. Phys. **B38**, 337 (1995) (Proc. Suppl.).
- [3] R. Shaefer and Q. Shafi, *Nature* **359**, 199 (1992); E. L. Wright *et al.*, *Astrophys. J.* **396**, L13 (1992); A. Klypin *et al.*, *ibid.* **416**, 1 (1993);
- [4] J. R. Primack *et al.*, Phys. Rev. Lett. **74**, 2160 (1995).
- [5] D. Caldwell and R. N. Mohapatra, Phys. Rev. **D48**, 3259 (1993); A. Ioannissyan and J.W.F. Valle, Phys. Lett. **B332**, 93 (1994); P. Bamert and C. P. Burgess, Phys. Lett. **B329**, 289 (1994); D. G. Lee and R. N. Mohapatra, Phys. Lett. **B329**, 463 (1994); A. S. Joshipura, Phys. Rev. **D51**, 1321 (1995); H. Minakata, hep-ph/9612259.
- [6] Particle Data Group, Phys. Rev. **D54**, 1 (1996).
- [7] J. T. Peltoniemi, D. Tommasini, and J. W. F. Valle, Phys. Lett. **B298**, 383 (1993).
- [8] J. T. Peltoniemi and J. W. F. Valle, Nucl. Phys. **B406**, 409 (1993).
- [9] D. Caldwell and R. N. Mohapatra, Phys. Rev. **D50**, 3477 (1994); G. M. Fuller, J. R. Primack and Y.-Z. Qian, Phys. Rev. **D52**, 1288 (1995); J. J. Gomez-Cadenas and M. C. Gonzales-Garcia, *Zeit. fur Physik* **C71**, 443 (1996); E. Ma and P. Roy, Phys. Rev. **D52**, R4780 (1995); E. Ma and J. Pantaleone, Phys. Rev. **D52**, R3763 (1995); R. Foot and R. R. Volkas, Phys. Rev. **D52**, 6595 (1995); Z. G. Berezhiani and R. N. Mohapatra, Phys. Rev. **D52**, 6607 (1995); E. J. Chun, A. S. Joshipura and A. Y. Smirnov, Phys. Lett. **B357**, 608 (1995).
- [10] C. Athanassopoulos, Phys. Rev. Lett. **77**, 3082 (1996); Phys. Rev. **C54**, 2708 (1996); J. E. Hill, Phys. Rev. Lett. **75**, 2654 (1995).
- [11] K. Kainulainen, J. Maalampi and J. T. Peltoniemi, Nucl. Phys. **B358**, 435 (1991).
- [12] S. P. Mikheyev and A. Yu. Smirnov, *Sov. Phys. JETP*, **64** (1986) 4; *Prog. Part. Nucl. Phys.* **23** 41 (1989).



- [13] X. Shi and G. Sigl, *Phys. Lett.* **B323**, 360 (1994).
- [14] G. Raffelt and G. Sigl, *Astropart. Phys.* **1**, 165, (1993).
- [15] S. A. Colgate and R. H. White, *Astrophys. J.* **143**, 626 (1966).
- [16] J. R. Wilson, *Numerical Astrophysics* ed. J. M. Centrella, J. M. Leblanc and R. L. Bowers (Boston, Jones and Bartlett), p.422 (1983);  
H. A. Bethe and J. R. Wilson, *Astrophys. J.* **295**, 14 (1985).
- [17] S. E. Woosley and E. Baron, *Astrophys. J.* **391**, 228 (1992);  
S. E. Woosley, *Astron. Astrophys. Suppl. Ser.* **97**, 205 (1993);  
S. E. Woosley and R. D. Hoffman, *Astrophys. J.* **395**, 202 (1992);  
B. S. Meyer *et al.*, *Astrophys. J.* **399**, 656 (1992);  
S. E. Woosley *et al.*, *Astrophys. J.* **433**, 229 (1994).
- [18] Y.-Z. Qian *et al.*, *Phys. Rev. Lett.* **71**, 1965 (1993);  
G. Sigl, *Phys. Rev.* **D51**, 4035 (1995).
- [19] H. Nunokawa *et al.*, *Phys. Rev.* **D54**, 4356 (1996);  
H. Nunokawa, A. Rossi and J. W. F. Valle, *Nucl. Phys.* **B482**, 481 (1996).
- [20] J. T. Peltoniemi, *Proc. Third Tallinn Symposium on Neutrino Physics*, Ed. I. Ots, J. Lõhmus, P. Helde and L. Palgi (Tartu, 1995) p. 103; hep-ph/9511323; hep-ph/9506228.
- [21] G. M. Fuller *et al.*, *Astrophys. J.* **322**, 795 (1987); G. M. Fuller, R. Mayle B.S. Meyer and J. R. Wilson, *Ap. J.* **389**, 517 (1992).
- [22] J. T. Peltoniemi, *Astron. & Astrophys.* **254**, 121 (1992).
- [23] S. P. Mikheyev and A. Yu. Smirnov, *Sov. J. Nucl. Phys.* **42**, 913 (1985).
- [24] S. P. Mikheyev and A. Yu. Smirnov, *Proc. of VI Moriond Workshop, '86 Massive Neutrinos'*, p. 355, ed. O. Facker and J. Tran Thanh Van, Edition Frontieres, 1986.
- [25] See for e.g., V. A. Kostelecky, J. Pantaleone and S. Samuel, *Phys. Lett.* **B315**, 46 (1993); S. Samuel, *Phys. Rev.* **D48**, 1462 (1993).
- [26] Y.-Z. Qian and G. M. Fuller, *Phys. Rev.* **D51**, 1479 (1995); G. Sigl, *Phys. Rev.* **D51**, 4035 (1995).
- [27] We acknowledge Y.-Z. Qian for providing us with the byproducts of the Wilson supernova code.
- [28] L. Landau, *Phys. Z. Sowjetunion* **2** 46 (1932);  
C. Zener, *Proc. R. Soc. London* **A137** 696 (1932).

- [29] W. C. Haxton, Phys. Rev. Lett. **57** 1271 (1986);  
 S. J. Parke, Phys. Rev. Lett. **57** 1275 (1986);  
 A. Dar et al., Phys. Rev. **D35** 3607 (1987).
- [30] J. Cooperstein, L. J. van den Horn and E.A. Baron, Astrophys. J. **309**, 653 (1986);  
 Astrophys. J. **315** 729 (1987).
- [31] K. Hirata *et al.*, Phys. Rev. Lett. **58**, 1490 (1987).
- [32] R. Bionta *et al.*, Phys. Rev. Lett. **58**, 1494 (1987).
- [33] Y. Suzuki, Talk given at Neutrino 96 conf., Helsinki, 1996, to appear in the Proc. Neutrino 96, Helsinki, ed. K. Huitu, K. Enqvist and J. Maalampi (World Scientific, Singapore, 1997).
- [34] G. T. Ewan, *et al.*, Sudbury Neutrino Observatory Proposal, SNO 87-12 (1987).
- [35] H. Nunokawa *et al.*, in preparation.
- [36] B. Achkar *et al.*, Nucl. Phys. **B434**, 503 (1995).
- [37] K. Kainulainen, Phys. Lett. **B237**, 440 (1990);  
 R. Barbieri and A. Dolgov, Nucl. Phys. **B349**, 743 (1991);  
 K. Enqvist, K. Kainulainen and M. Thomson, Nucl. Phys. **B373**, 498 (1992);  
 J. M. Cline, Phys. Rev. Lett. **68**, 3137 (1992);  
 X. Shi, D. Schramm and B. D. Fields, Phys. Rev. **D48**, 2563 (1993);  
 C. Y. Cardall and G. M. Fuller, Phys. Rev. **D54**, 1260 (1996).
- [38] R. Foot, M. J. Thomson and R. R. Volkas, Phys. Rev. **D53**, 5349 (1996);  
 R. Foot, and R. R. Volkas; UM-P-96/81, RCHEP-96/09, hep-ph/9610229.
- [39] C. J. Copi, D. N. Schramm and M. S. Turner, Phys. Rev. Lett. **75**, 3981 (1995);  
 P. J. Kernan and S. Sarkar, Phys. Rev. **D54**, 368 (1996).  
 for a more extreme view on this subject see e.g. N. Hata *et al.*, Phys. Rev. Lett. **75**,  
 3977 (1995), who argued that  $N_\nu \simeq 2.1$ .
- [40] R.F. Carswell, M. Rauch, R.J. Weynman et al., *MNRAS* **268** L1(1994); A. Songalia,  
 L.L. Cowie, C. Hogan and M. Rugers, *Nature* **368** 599 (1994).
- [41] D. Tytler and X.M. Fan, *Bull. Am. Astr. Soc.* **26** 1424 (1994).

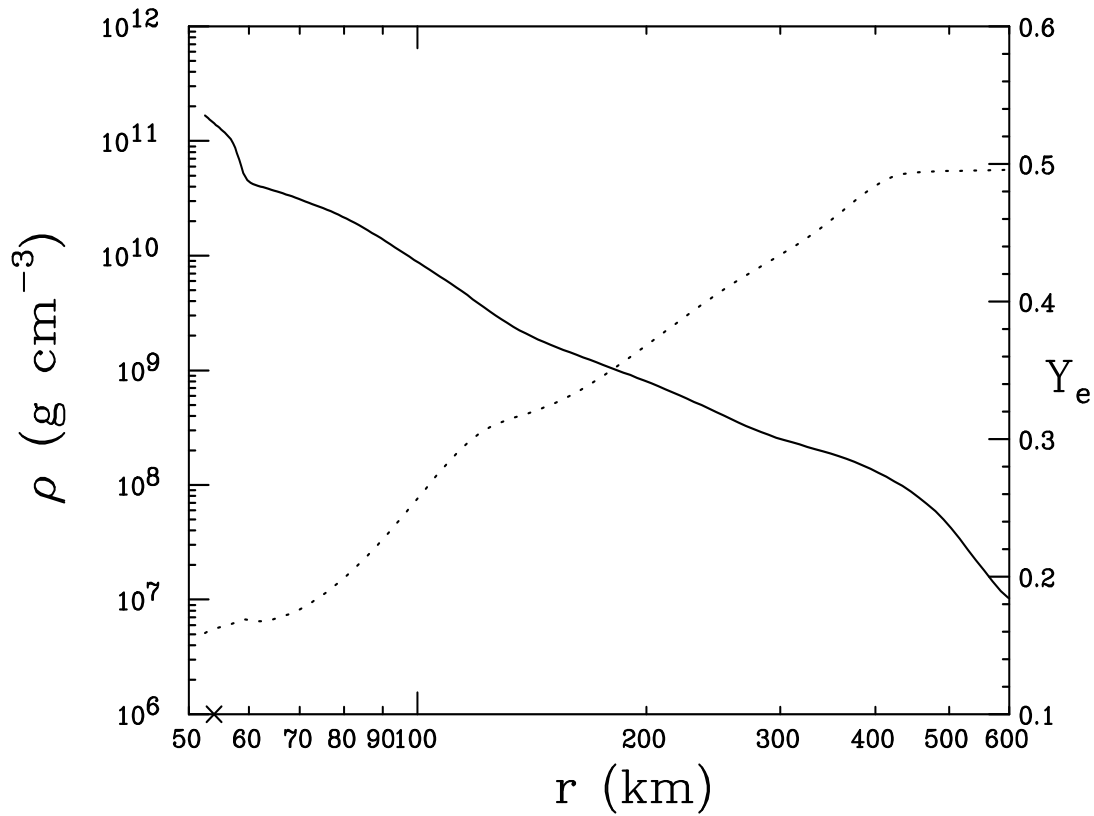


Fig. 1a: Typical matter density (solid line) and  $Y_e$  (dotted line) profiles versus the radial distance from the center of the star, in Wilson's numerical supernova model at  $t = 0.15$  s after the core bounce. The diagonal cross indicates the position of the surface of the neutrinosphere.

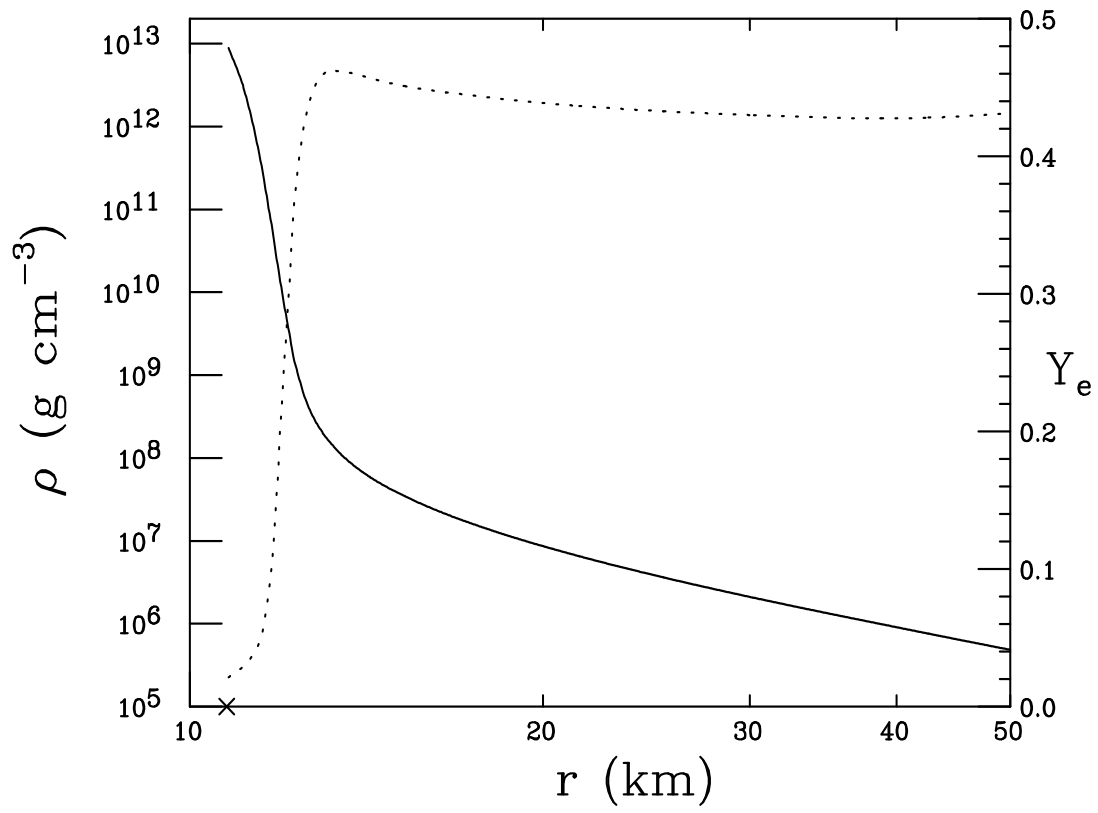


Fig. 1b: Same as in Fig. 1a but for  $t \sim 6$  s after the core bounce.

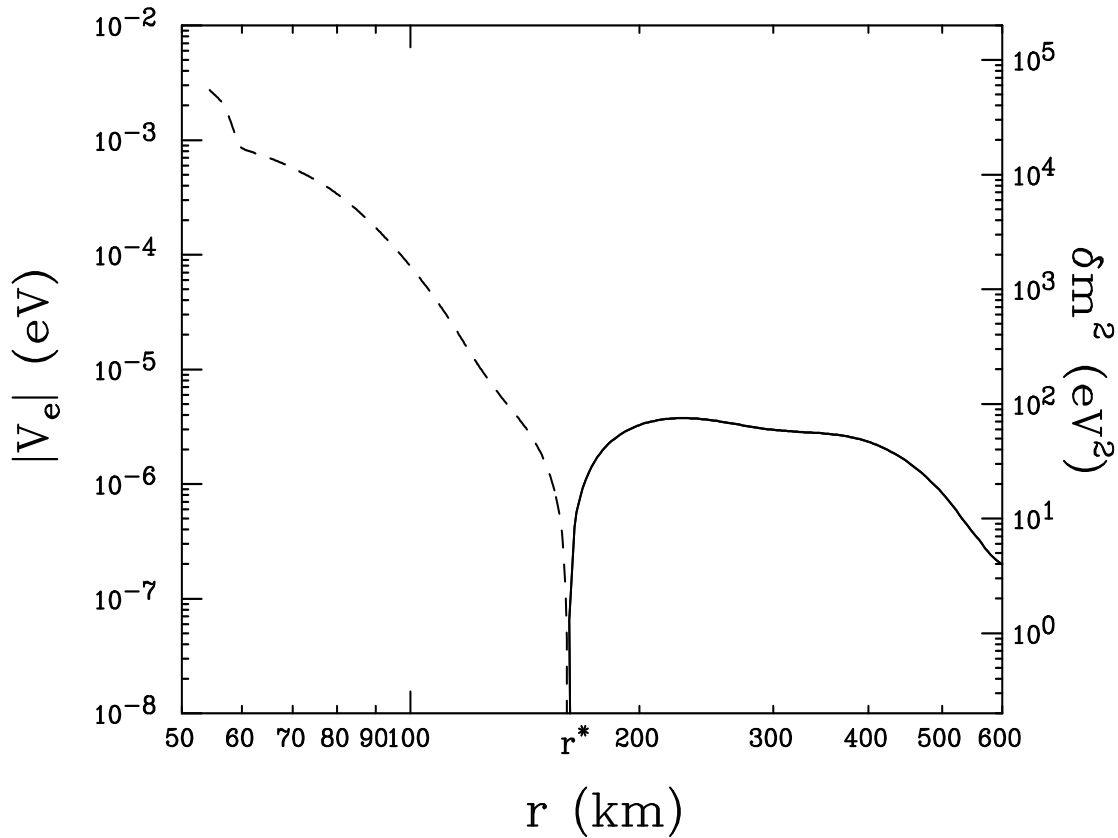


Fig. 2a: The modulus of the matter potential  $V_e$  in eq. (3) versus the radial distance  $r$  from the center of the star. This is obtained using the matter density and  $Y_e$  profiles in Fig. 1a, at  $t < 1$  s after the core bounce. The solid and dashed lines correspond to positive and negative potential, respectively, and the position where  $V_e = 0$  is denoted by  $r^*$ . We also indicate, in the right ordinate, the  $\delta m^2$  values for which a  $E = 10$  MeV neutrino undergoes resonant conversion, for the corresponding value of  $|V_e|$  on the left ordinate (small mixing angle is understood).

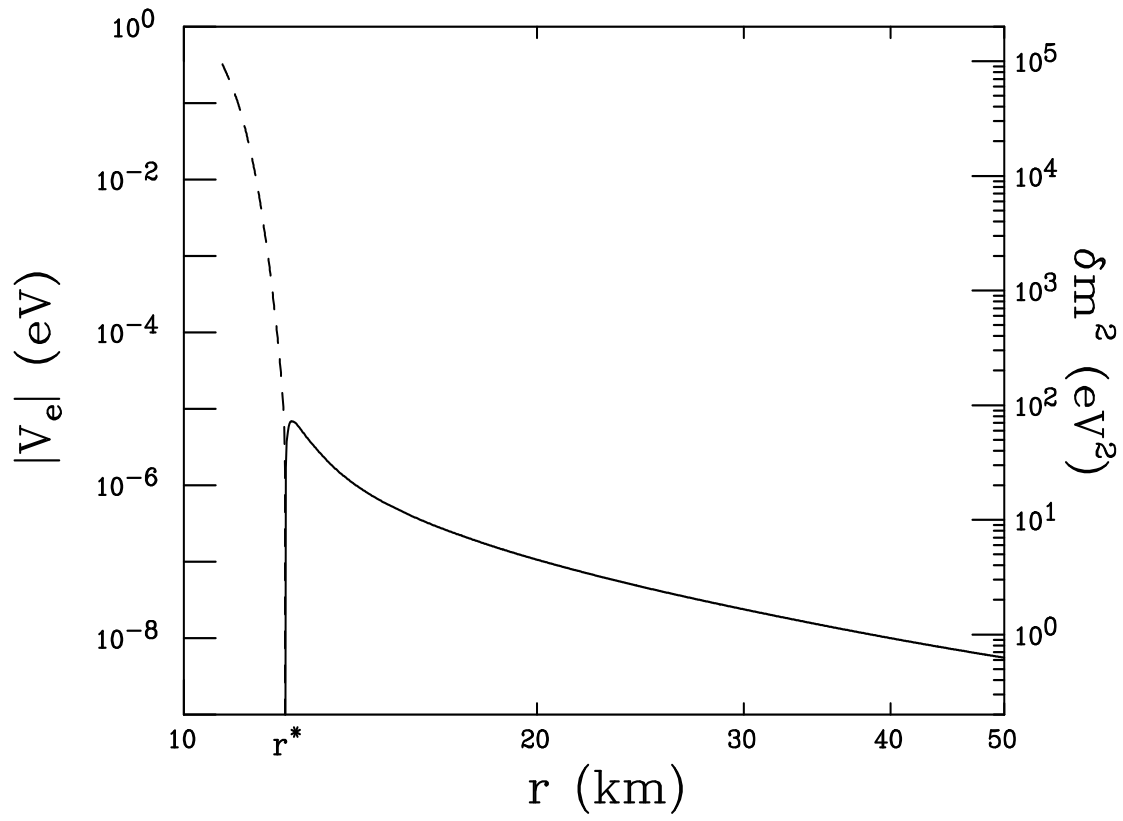


Fig. 2b: Same as in Fig. 2a but for  $t > 1$  s after the core bounce.

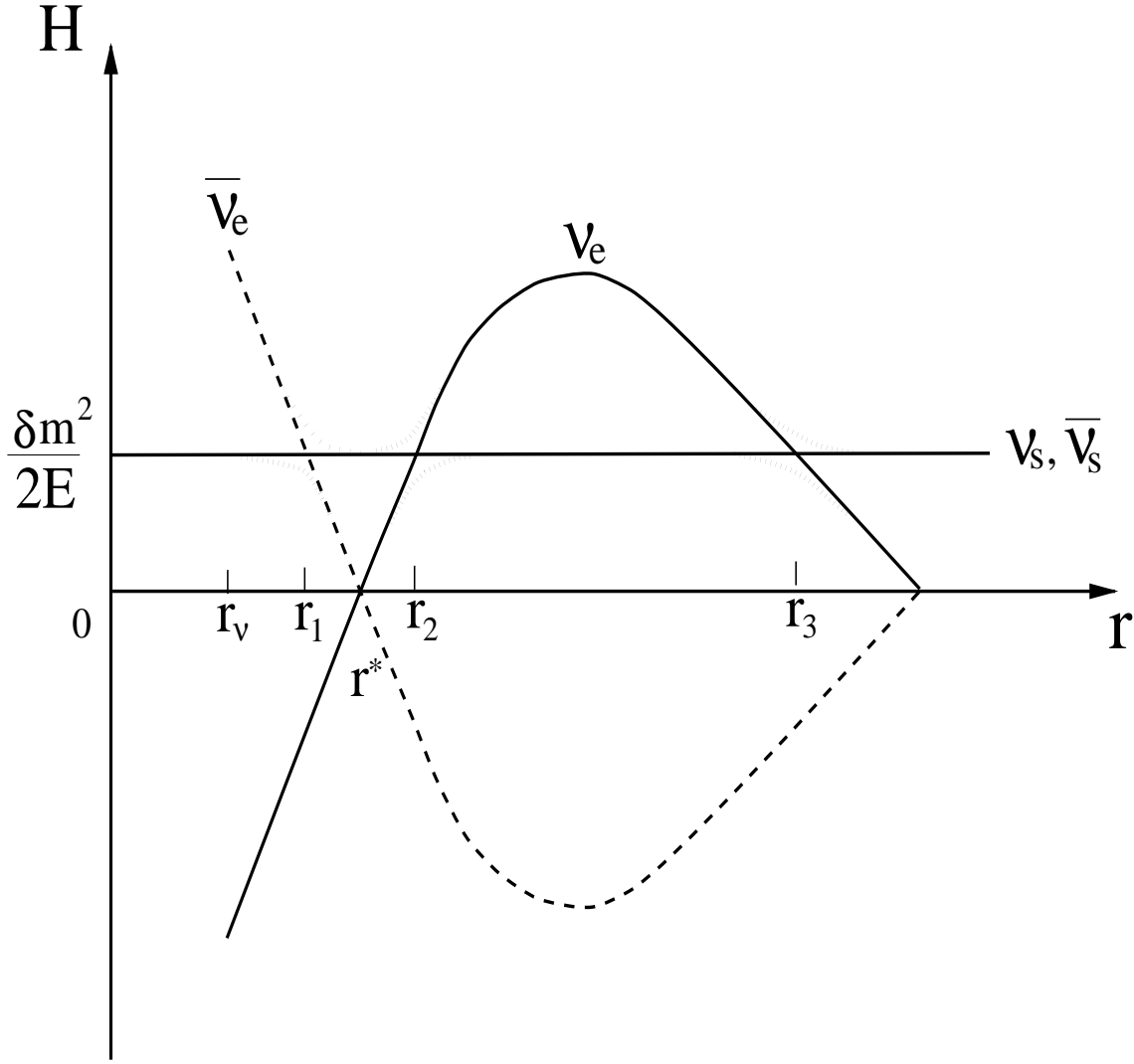


Fig. 3: Schematic figure illustrating the level crossings for  $\nu_e - \nu_s$  and  $\bar{\nu}_e - \bar{\nu}_s$  system. The energy levels of  $\nu_e$  (solid line),  $\bar{\nu}_e$  (dashed line) and  $\nu_s, \bar{\nu}_s$  (horizontal line) are given as functions of the stellar radius. The positions where  $\bar{\nu}_e \rightarrow \bar{\nu}_s$  and  $\nu_e \leftrightarrow \nu_s$  resonances occur are indicated by  $r_1, r_2$  and  $r_3$ , respectively.

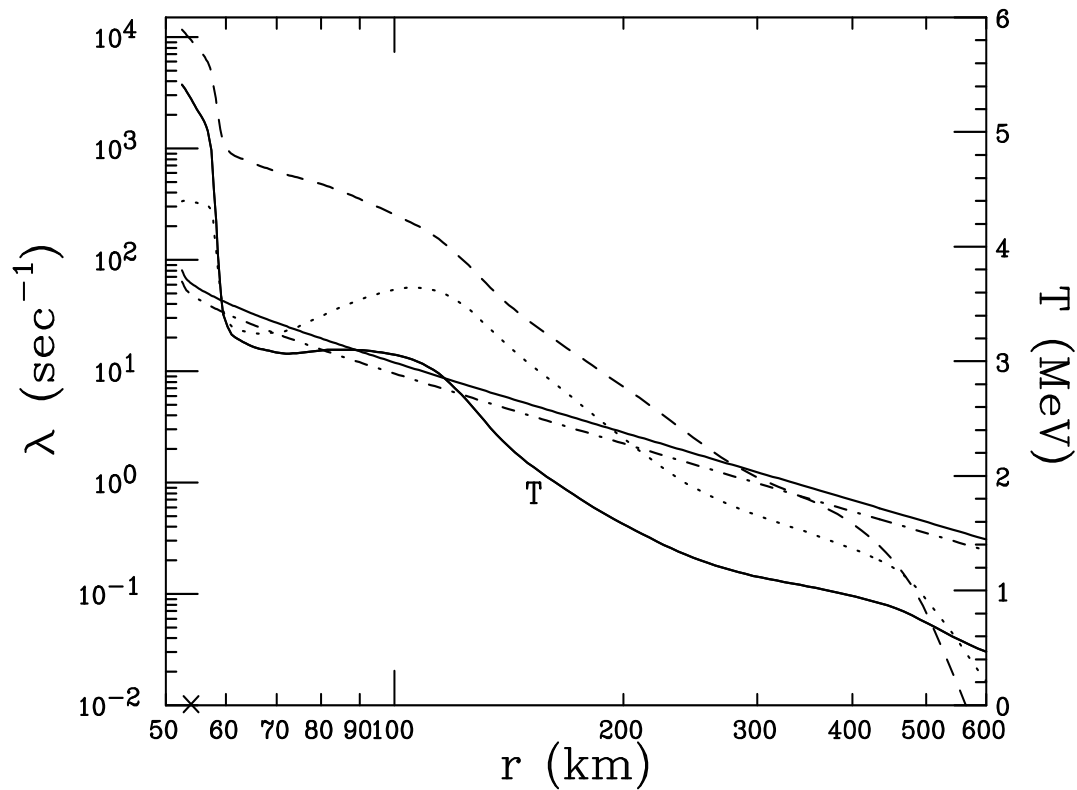


Fig. 4a: Main neutrino reaction rates (left ordinate) versus the radial distance from the stellar center at  $t < 1$  s after the core bounce:  $\nu_e n \rightarrow p e^-$  (solid curve),  $\bar{\nu}_e p \rightarrow n e^+$  (dot-dashed curve),  $e^- p \rightarrow \nu_e n$  (dashed curve) and  $e^+ n \rightarrow \bar{\nu}_e p$  (dotted curve). The temperature profile (right ordinate) is also shown by the solid line (labelled  $T$ ). We assume a neutrino (and anti-neutrino) luminosity of  $L_\nu = 10^{52}$  ergs/s.



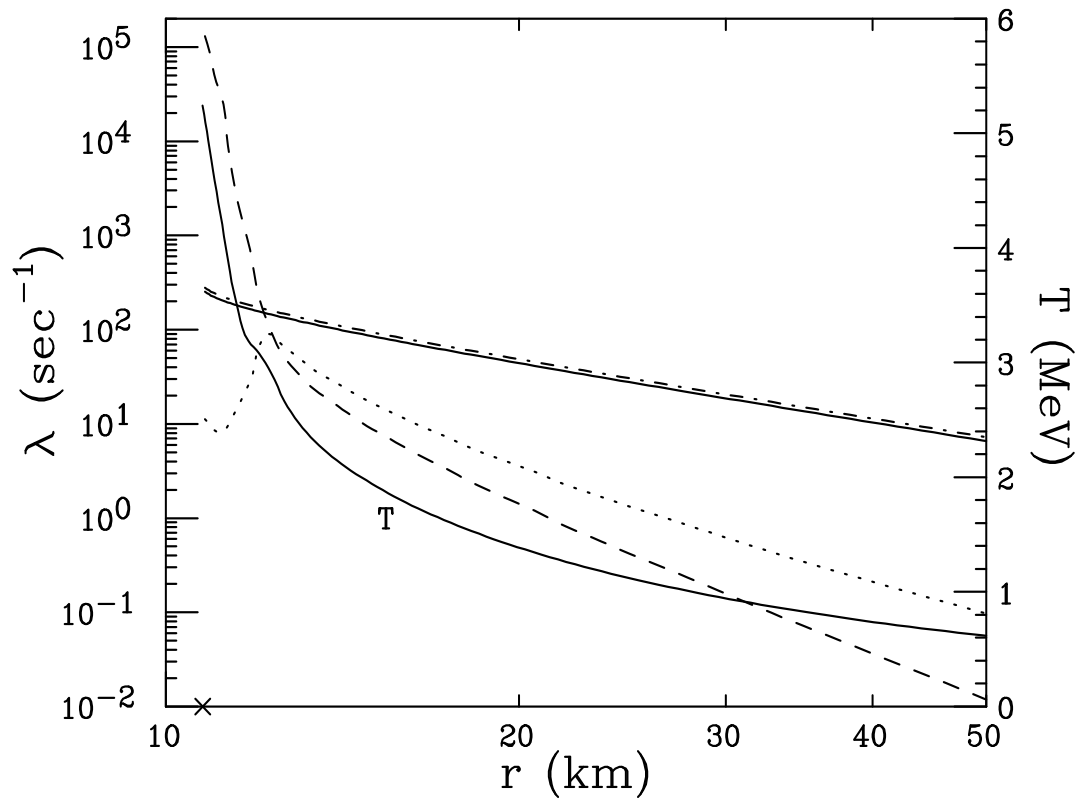


Fig. 4b: Same as in Fig. 4a but for  $t > 1$  s after the core bounce.

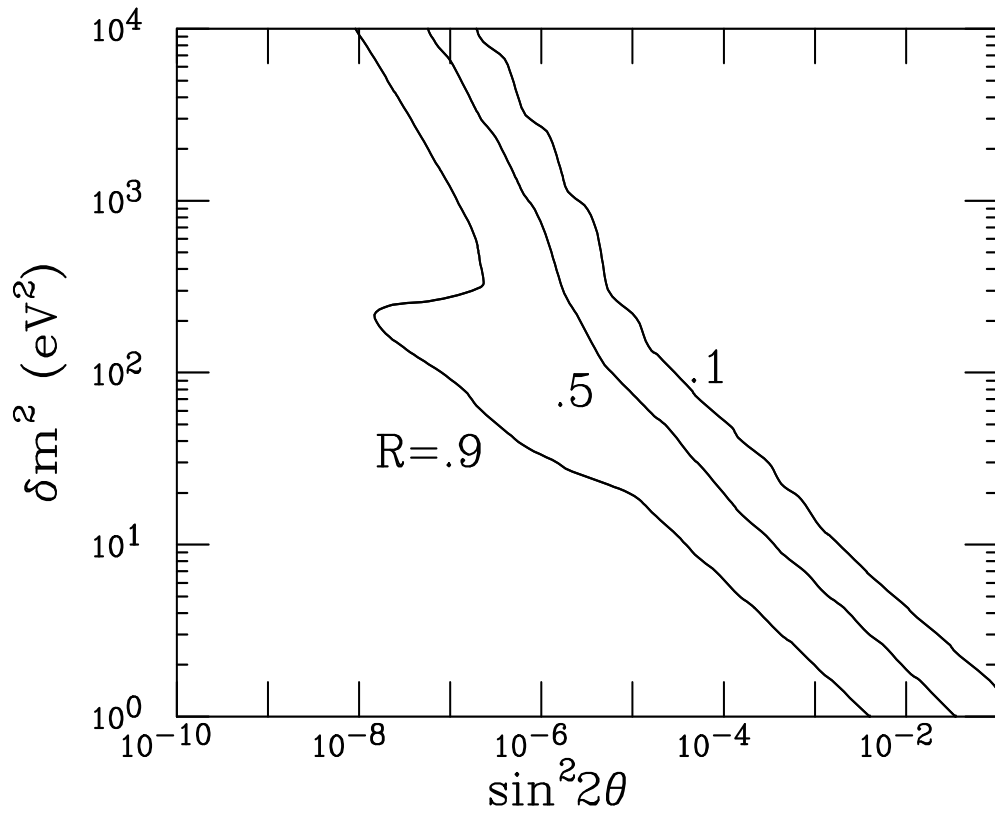


Fig. 5: Contour plot of the ratio  $R$  of the neutrino energy deposition behind the shock wave in the presence of conversions into sterile neutrinos, versus the case without conversions, as defined in eq. (15).

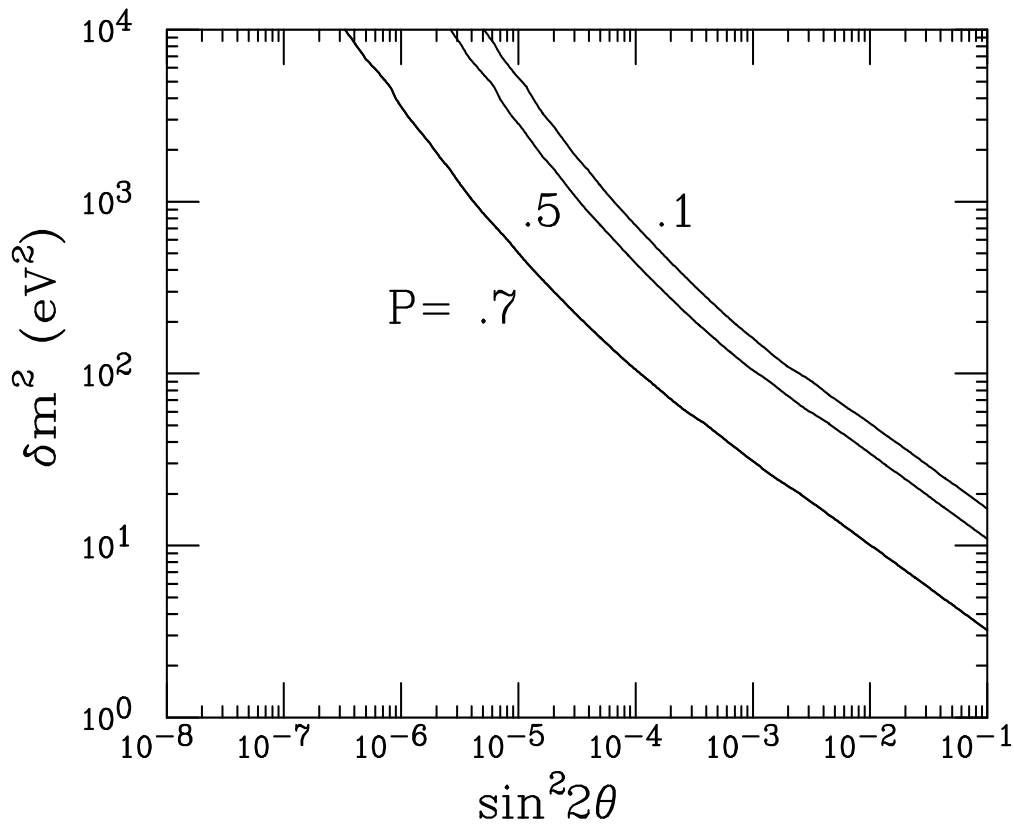


Fig. 6: Contour plots of the survival probability  $P$  (figures at the curve) for the  $\bar{\nu}_e \rightarrow \bar{\nu}_s$  conversion at  $t > 1$  s p.b. The region to the right of the curves can be excluded by the observation of the SN1987A  $\bar{\nu}_e$  signal.

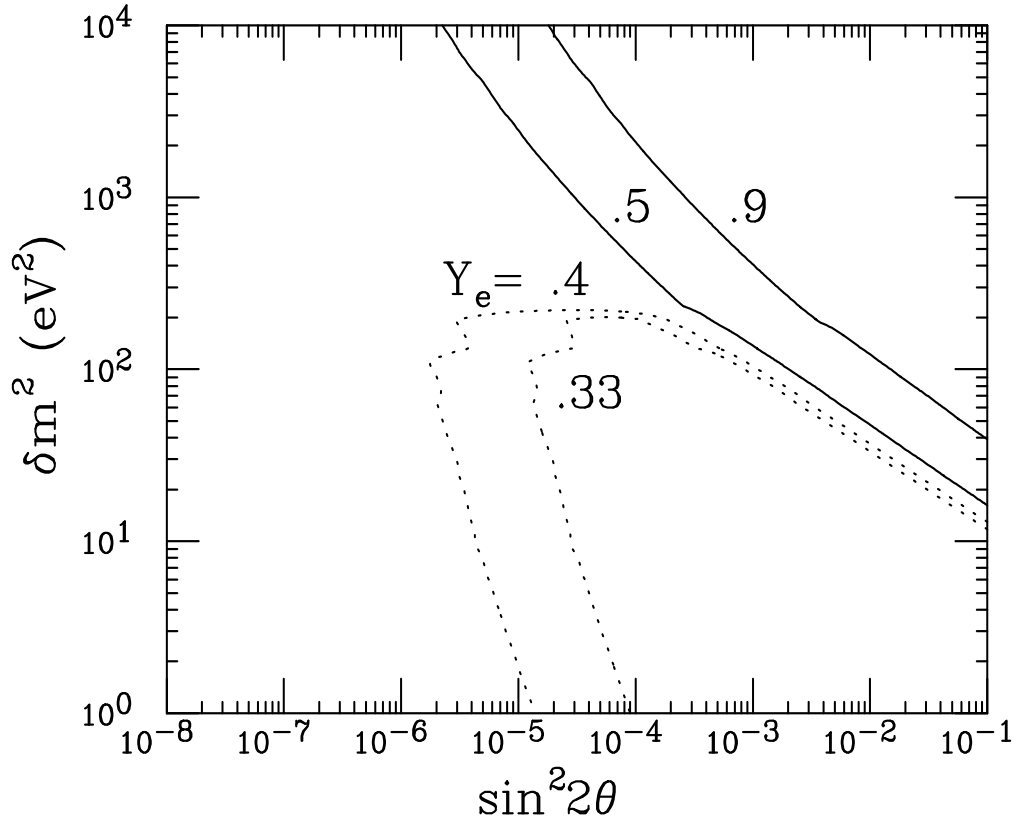


Fig. 7: Contour plots for the electron concentration  $Y_e$  (figures at the curves) taking into account  $\bar{\nu}_e \rightarrow \bar{\nu}_s$  and  $\nu_e \rightarrow \nu_s$  conversions at  $t > 1$  s p.b. The region to the right of the solid line labelled 0.5 is ruled out by the condition  $Y_e < 0.5$  necessary for  $r$ -process nucleosynthesis to occur. For the parameter region inside the  $Y_e = 0.4$  dotted contour  $r$ -process nucleosynthesis can be enhanced.